An Interactive DMS Emissions Scheme for the Unified Model

Andy Jones and David L. Roberts

February 2004

Met Office

An Interactive DMS Emissions Scheme for the Unified Model

Andy Jones and David L. Roberts

1 Introduction

The impact of anthropogenic aerosols is one of the factors contributing the most uncertainty to predictions of climate change (IPCC 2001). Aerosols can affect the radiative balance of the planet by directly scattering and/or absorbing shortwave (solar) and longwave (terrestrial) radiation, the so-called "direct effect". Certain aerosols, which due to their physical and chemical properties are capable of forming cloud condensation nuclei (CCN), may also affect climate *via* "indirect" effects, by modifying cloud properties (Twomey 1974, Albrecht 1989). The radiative effects of aerosols in general act to cool the planet, and indeed the indirect effects, which are thought to have a greater impact than the direct effect, may offset a sizable fraction of the warming due to increases in greenhouse gases. Unfortunately, these effects are also the most uncertain.

For the direct effect, the radiative impact of a given anthropogenic increase in aerosol amount is more or less linearly related to the size of the increase. This is not, however, true for the indirect effects, where cloud properties are non-linearly related to aerosol concentrations. This means that the impact of a given change in aerosol concentration (*via* indirect effects) depends on the initial aerosol concentration. This underpins the idea of cloud "susceptibility" (Twomey 1991), whereby clouds in unpolluted regions are more strongly affected by aerosol changes than clouds in more polluted areas.

Changes in the concentration of aerosols which act as CCN affects the number concentration of cloud droplets (N_d), which in turn affects the size distribution of cloud droplets. A measure of this is cloud droplet effective radius, r_e:

$$r_e = \sqrt[3]{\frac{3\,q_c\,\rho_o}{4\pi\,\rho_w\,\kappa\,N_d}} \tag{1}$$

where q_c is the cloud liquid water mixing ratio, ρ_o and ρ_w the densities of air and water respectively, and κ is a quantity related to the spectral dispersion of the cloud droplet spectrum (Martin *et al.* 1994). Effective radius may be related to cloud optical depth (τ) by:

$$\tau = \frac{3\,W}{2\,\rho_w\,r_e} \tag{2}$$

where W is the cloud liquid water path (Stephens 1978). This may be related to a simple measure of cloud albedo (α) using an expression based on Bohren (1980):

$$\alpha = \frac{\tau(1-g)}{1.5 + \tau(1-g)} \tag{3}$$

where g is the assymetry parameter (assumed to be 0.85). For an idealised cloud of thickness 300m, a liquid water mass mixing ratio of 3×10^{-4} kg kg^{-1} and a value of κ of 0.8 (appropriate for a maritime cloud), the relation between N_d and cloud albedo is shown in Figure 1; the most sensitive region is clearly for low values of N_d. In terms of predicting climate change, this means that in order to assess the potential effect of anthropogenic aerosol changes, it is important that the natural, unperturbed aerosol distribution is well simulated.

Sulphate aerosols are an important component of atmospheric CCN. Over continental areas, the major source of sulphate aerosol is anthropogenic: the burning of fossil fuels results in the emission of sulphur dioxide (SO_2) which is oxidised to form sulphate aerosols. However, over ocean areas remote from pollution sources, the major source of sulphate aerosols is natural: marine phytoplankton emit dimethylsulphide (DMS, CH_3SCH_3) which is subsequently oxidised to form sulphate. Supplemented by sea-salt from the ocean surface, sulphate from DMS is the major source of CCN over ocean areas. Given that over 70% of the planet's surface is ocean, simulating the natural, unperturbed aerosol distribution requires that DMS emissions are well simulated.

2   DMS emissions in the Unified Model

As standard, the Unified Model has used climatologies of DMS emissions compiled by Kettle *et al.* (1999). This is based on a climatology of seawater DMS concentrations based on measurements made by many workers at thousands of locations around the world. This are then combined in Kettle *et al.*'s model with climatological surface windspeed and sea-surface temperature (SST) distributions, and with parameterizations of sea-air exchange, to produce a climatology of emissions at monthly-mean resolution. A disadvantage of this approach is that climatological quantities are used three times: the concentration of DMS in seawater, the surface windspeed and SSTs. Another problem is the fact that the sea-air exchange rates for DMS are poorly known (*e.g.* Nightingale *et al.* 2000). Consequently two different DMS emission climatologies from Kettle *et al.* have at times been used, one based upon the exchange parameterization of Wanninkhof (1992) and the other on that of Liss & Merlivat (1996).

An idea of the significance of correctly simulating the natural "background" CCN distribution can be obtained from the results of Jones *et al.* (2001). Their

study showed that estimates of annual-mean indirect forcing in the HadAM4 model could be reduced by over 25% if the DMS emissions climatology based on the Wanninkhof (1992) parameterization was used, compared with using the one based on the Liss & Merlivat (1996) scheme.

3   The interactive scheme

To attempt to improve the simulation of DMS emissions, a more interactive emissions scheme has been introduced in the new HadGEM1 model. It is "more interactive" in that it uses Kettle *et al.*'s distributions of seawater DMS concentration directly with instantaneous model winds and SSTs. This is desirable because the DMS flux climatology implicitly includes the surface windspeed and SST climatologies used in Kettle *et al.*'s model, which are unlikely to be identical to those of HadGEM1.

The ratio of the kinematic viscosity of a liquid to the molecular diffusivity of a gas therein is known as the Schmidt number (Sc) for that gas in the given liquid. If the ratio of the Schmidt numbers of two gases is known, then the ratio of their mass transfer (or "piston") velocities (k) is also known:

$$k_1/k_2 = (Sc_1/Sc_2)^n. \tag{4}$$

Different sea-air exchange parameterization schemes attempt to give expressions for k for "reference" gases of specified Schmidt number, which may then be combined with the Schmidt number of the required gas, in this case DMS, to determine its piston velocity:

$$k_{DMS} = k_{ref}(Sc_{DMS}/Sc_{ref})^n. \tag{5}$$

The Schmidt number for DMS is obtained following Saltzman *et al.* (1993):

$$Sc_{DMS} = 2674.0 - 147.12\,T_c + 3.726\,T_c^2 - 0.038\,T_c^3 \tag{6}$$

where T_c is sea-surface temperature in degrees Celsius.

The interactive scheme has been implemented to allow a choice of one of three standard sea-air exchange parameterizations, that of Liss & Merlivat (1986), Wanninkhof (1992) and Nightingale *et al.* (2000). Windspeed at 10m above the sea-surface (u_{10}) is used by the schemes to parameterize k_{ref}, and the Schmidt number exponent n is either specified or also given as a function of windspeed.

3.1 Liss & Merlivat

This parameterization provides different expressions depending on the wind-speed; for $u_{10} \leq 3.6 \text{ms}^{-1}$:

$$k_{600} = 0.17 \, u_{10} \, ; \qquad n = -2/3. \qquad (7)$$

For $3.6 < u_{10} \leq 13 \text{ms}^{-1}$:

$$k_{600} = 2.85 \, u_{10} - 9.65 \, ; \qquad n = -1/2; \qquad (8)$$

and for $u_{10} > 13 \text{ms}^{-1}$:

$$k_{600} = 5.9 \, u_{10} - 49.3 \, ; \qquad n = -1/2. \qquad (9)$$

3.2 Wanninkhof

This scheme differs from the other two in that its reference Schmidt number is 660, not 600:

$$k_{660} = 0.31 \, u_{10}^2 \, ; \qquad n = -1/2. \qquad (10)$$

3.3 Nightingale *et al.*

This scheme is written in terms of 10m windspeed normalised to a neutral profile, but as that is how 10m windspeed is calculated in the new routine anyway, this difference is irrelevant:

$$k_{600} = 0.222 \, u_{10}^2 + 0.333 \, u_{10} \, ; \qquad n = -1/2. \qquad (11)$$

*

These equations provide the reference piston velocity and the Schmidt number exponent which can then be used in equation (5) to calculate k_{DMS}. This may then be used to calculate the flux of DMS (F_{DMS}) from the concentration of DMS in seawater (C_{DMS}). Piston velocity is conventionally calculated in units of cm hour^{-1}, and the Kettle *et al.* climatology gives C_{DMS} in nanomoles per litre of S as DMS, so to get F_{DMS} in kg [S] m^{-2} s^{-1} as required we use:

$$F_{DMS} = (8/9) \times 10^{-13} \, k_{DMS} \, C_{DMS} \qquad (12)$$

4 Experiments

The performance of the interactive DMS emission scheme was evaluated using a developmental version of HadGAM1, the atmospheric component of the new climate model HadGEM1, at Unified Model version 5.4. The experiments were conducted using climatological sea-surface temperature and sea-ice distributions representative of present-day conditions. Both sulphate and sea-salt aerosols, and their direct and indirect effects, were simulated — see Jones *et al.* (2001) for details of the schemes. Four experiments were performed: the first used the standard Unified Model approach of using non-interactive, climatological DMS emission fields from Kettle *et al. via* the Wanninkhof sea-air exchange scheme. The other three experiments used the interactive scheme, each using a different one of the sea-air exchange schemes described in Section 3. Each experiment was run for 5 years following a (discarded) 3-month spinup period.

5 Results

As described in the introduction, DMS is important because of its contribution to the distribution of sulphate aerosol (which can act as CCN), and so it is in these terms that the performance of the simulations was evaluated.

Annual mean concentrations of dry sulphate mass in the lowest model layer are compared with near-surface measurements in Figure 2(a-d). The upper plot in each panel compares the 5-year mean model values against long-term means from selected stations of the European Monitoring and Evaluation Programme (EMEP) network in Europe; the lower plot compares the model against selected stations from the University of Miami database (D. L. Savoie and J. M. Prospero, personal communication, 1999). The value at the model gridpoint closest to the measurement station is taken in each case. The stations in the EMEP network, being European, will clearly be heavily influenced by anthropogenic sources of sulphate, and so might not be expected to be significantly influenced by DMS emissions. The sites from the University of Miami database, on the other hand, are remote from sources of pollution and are from various coastal and oceanic sites around the globe. Sulphate concentrations at these sites are much more likely to be dependent on the level of DMS emissions.

Figure 2(a) shows the results from the standard model with prescribed climatological DMS emissions; the lower plot indicates a tendency for the model to over-predict sulphate concentrations in areas remote from anthropogenic

pollution sources. Figures 2(b), (c) and (d) show the results from the inter-
active scheme using the parameterizations of Liss & Merlivat, Wanninkhof
and Nightingale *et al.* respectively. As mentioned above, it is not too sur-
prising that the comparison against the EMEP data is little changed in any
of the experiments: over Europe the sulphate concentration is dominated by
anthropogenic sources. However, comparison against the University of Miami
measurements shows a noticeable improvement in all cases using interactive
DMS emissions compared with using the climatology. The correlation coeffi-
cients of all three "interactive" experiments against the University of Miami
measurements are very similar, so based on a somewhat subjective analysis,
the interactive scheme using the Wanninkhof (1992) scheme (Fig. 2c) was
preferred and selected for use in the HadGEM1 model (although the other
schemes are still available as options).

Figure 3(a-d) shows the December-February and June-August seasonal dis-
tributions of DMS emissions from the simulations using the Kettle *et al.* cli-
matology and from the interactive scheme with the Wanninkhof parameteri-
zation. The larger climatological emissions responsible for the overestimate of
sulphate seen in Figure 2 are evident, but the distribution of the emissions, as
well as their magnitude, is also different. Both have their maximum emissions
in the Southern Ocean during austral summer (Figs.3a & 3b), but the clima-
tology has a much wider zone of high emissions than the interactive scheme,
the latter being both narrower in latitudinal extent and also much closer to
the Antarctic ice-edge. The southern hemisphere emissions also differ in their
meridional distribution, with the climatology having highest values between
approximately 90°E and the dateline, whereas the interactive scheme produces
its highest emissions just to the east of the Drake Passage. (Neither of these
features is clear in Figure 3 because of the common contour interval chosen.)
The climatology also has prominent maxima in both the North Pacific and
North Atlantic during December-February, features clearly absent in the in-
teractive simulation.

The areas of highest DMS emission have moved northwards in June-August
(Figs.3c and 3d). In the climatology, however, this is due more to the ab-
sence of the maximum in the Southern Ocean than to any changes in the
North Pacific and North Atlantic, where the emissions are similar to those in
December-February. In contrast, the interactive scheme shows a more pro-
nounced seasonal cycle in these areas, especially the North Atlantic. Both
have a maximum off the horn of Africa related to monsoon winds.

To assess the impact of using the interactive scheme on the radiative forcing
by sulphate aerosols, two further 5-year experiments were performed. These
used only natural ("pre-industrial") sources of sulphate aerosol precursors,

one using the standard DMS emissions climatology, the other the interactive scheme. The difference in the 5-year mean top-of-atmosphere net radiation balance between these pre-industrial experiments and their respective "modern-day" counterparts (*i.e.* those which used natural plus anthropogenic SO_2 emissions) is a measure of the radiative impact of anthropogenic sulphate aerosols in that model configuration. This is the total sulphate aerosol forcing (as both indirect and direct effects were included in these simulations), although the major change will be *via* the indirect effects, as it is these which are affected by the pre-industrial "background" sulphate levels. The global annual-mean total sulphate forcing in the standard experiment using the DMS emissions climatology was -1.45 ± 0.22 Wm^{-2}; this increases to -1.53 ± 0.19 Wm^{-2} when the interactive DMS emissions scheme is used, due to the lower background sulphate levels produced by the scheme.

6   Discussion and Conclusion

The new scheme, which incorporates a more physical dependence of DMS emissions on windspeeds and sea-surface temperatures, appears to perform better than using a non-interactive emissions climatology. This improvement is ascribed to the use of instantaneous model winds in the interactive scheme, as opposed to dependence on a windspeed climatology implicit in the non-interactive approach. It is not clear, however, whether the improved results are due to the windspeeds used being "instantaneous", as opposed to the time-averaged ones underlying the DMS climatology, or are due to deficiencies in the windspeed climatology other than issues of time-averaging.

Including the dependency of DMS emission rates on surface windspeed and sea-surface temperatures in HadGEM1 improves the physical basis of this aspect of the model. The inclusion of the inter-relation of these quantities means that a mechanism for feedbacks between them is now possible. Although climatological sea-surface temperatures were used in the tests described above, this will not be the case in the HadGEM1 model configuration to be used for the next set of large climate change experiments, where such feedbacks may be important.
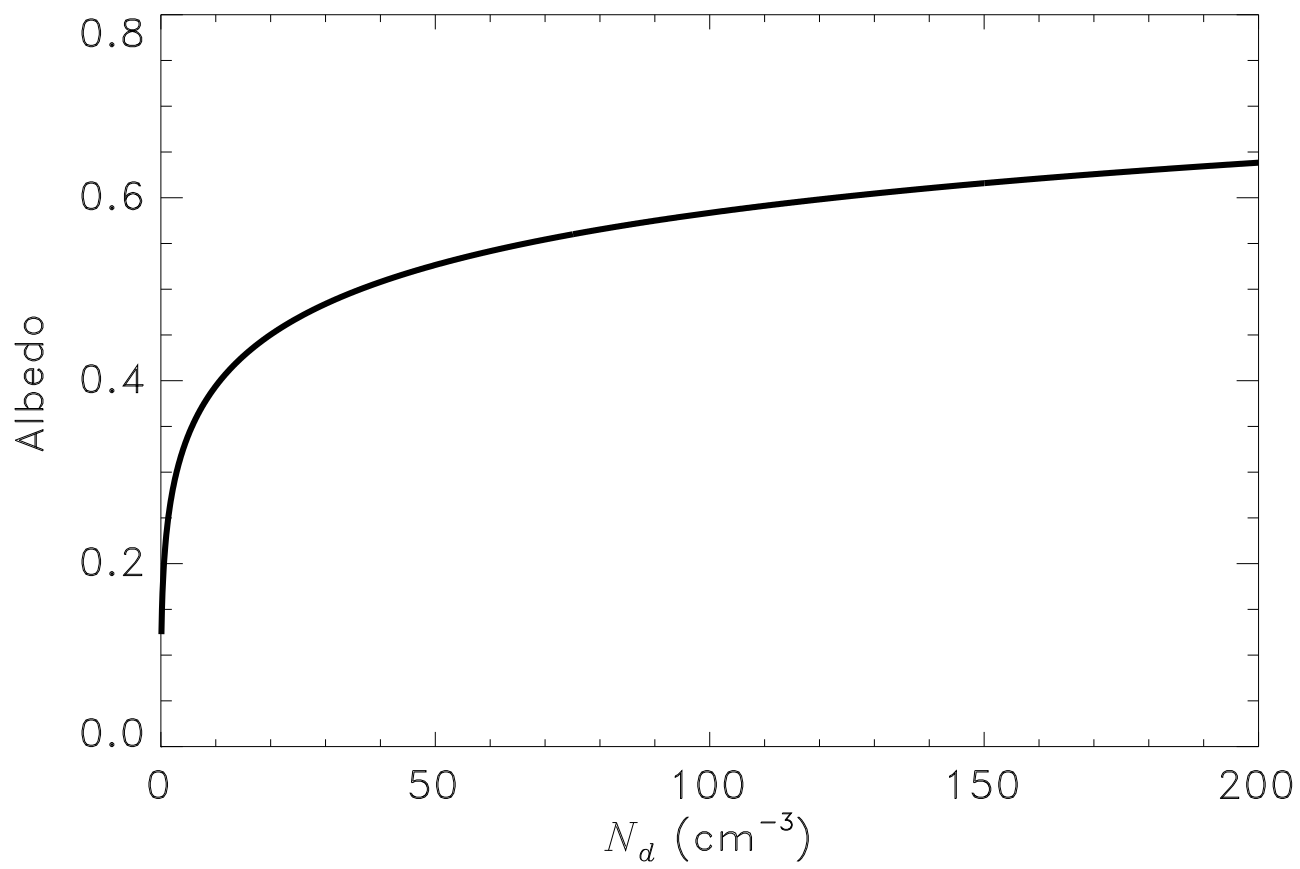
References

Albrecht, B. A., 1989. Aerosols, cloud microphysics and fractional cloudiness. *Science*, **245**, 1227-1230

Bohren, C. F., 1980. Multiple scattering of light and some of its observable consequences. *Amer. J. Phys.*, **55**, 524-533

IPCC, 2001. *Climate Change 2001: The Scientific Basis*, edited by J. T. Houghton *et al.*, Cambridge University Press, Cambridge, UK

Jones, A., Roberts, D. L., Woodage, M. J. and Johnson, C. E., 2001. Indirect sulphate aerosol forcing in a climate model with an interactive sulphur cycle. *J. Geophys. Res.*, **106**, 20293-20310

Kettle, A. J., *et al.*, 1999. A global database of sea surface dimethylsulfide (DMS) measurements and a procedure to predict sea surface DMS as a function of latitude, longitude and month. *Global Biogeochem. Cycles*, **13**, 399-444

Liss, P. S. and Merlivat, L., 1986. Air-sea gas exchange rates: Introduction and synthesis. In *The Role of Air-Sea Exchange in Geochemical Cycling*, edited by P. Buat-Menard, D. Reidel, Dordrecht, The Netherlands

Martin, G. M., Johnson, D. W., and Spice, A., 1994. The measurement and parameterisation of effective radius of droplets in warm stratocumulus clouds. *J. Atmos. Sci.*, **51**, 1823-1842

Nightingale, P. D., Malin, G., Law, C. S., Watson, A. J., Liss, P. S., Liddicoat, M. I., Boutin, J. and Upstill-Goddard, R. C., 2000. In situ evaluation of air-sea gas exchange parameterizations using novel conservative and volatile tracers. *Global Biogeochem. Cycles*, **14**, 373-387

Saltzman, E. S., King, D. B., Holmen, K. and Leck, C., 1993. Experimental determination of the diffusion coefficient of dimethylsulfide in water. *J. Geophys. Res.*, **98**, 16481-16486

Stephens, G. L., 1978. Radiation profiles in extended water clouds, II: Parameterization schemes. *J. Atmos. Sci.*, **35**, 2123-2132

Twomey, S. A., 1974. Pollution and the planetary albedo. *Atmos. Environ.*, **8**, 1251-1256

Twomey, S., 1991. Aerosols, clouds and radiation. *Atmos. Environ. Part A*, **25**, 2435-2442

Wanninkhof, R., 1992. Relationship between wind speed and gas exchange over the ocean. *J. Geophys. Res.*, **97**, 7373-7382
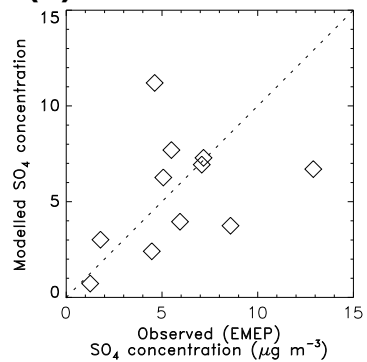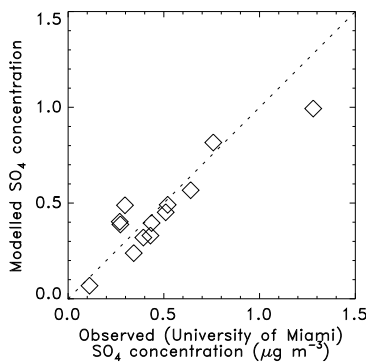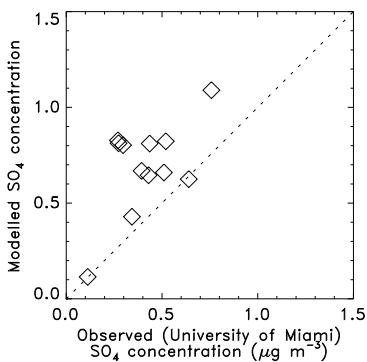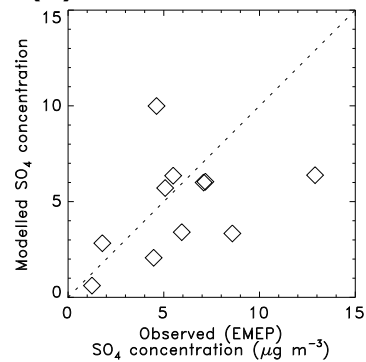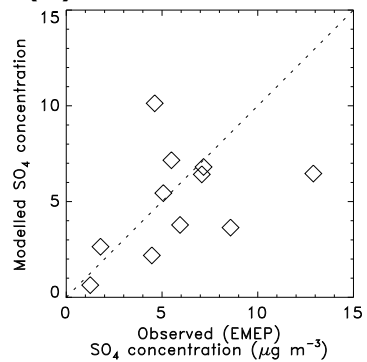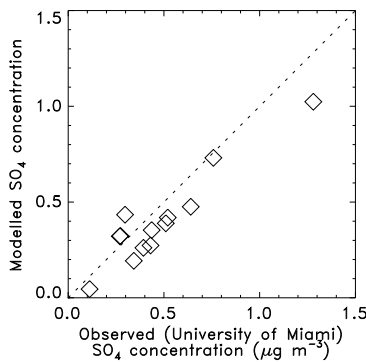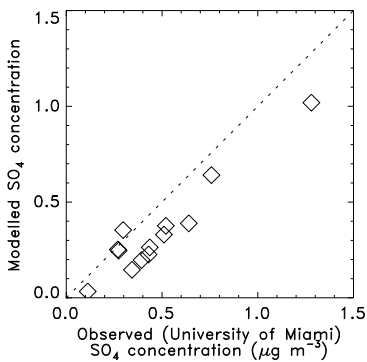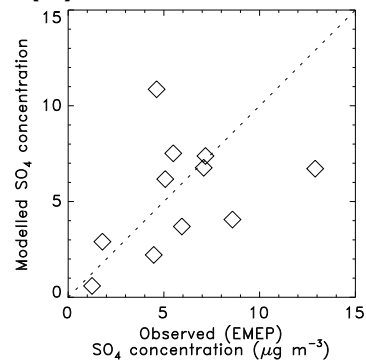
Fig. 1

Fig.2(a)

Fig.2(c)

Fig.2(b)

Fig.2(d)

Fig.3(a)
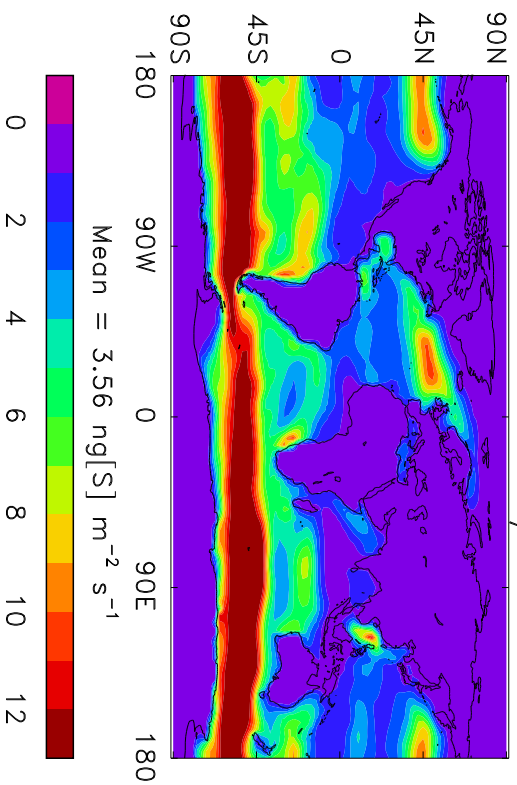Climatological DMS emisisons (ng[S] m $^{-2}$ s $^{-1}$)
December–February mean

Mean = 3.56 ng[S] m $^{-2}$ s $^{-1}$

Fig.3(b)
Interactive DMS emisisons (ng[S] m $^{-2}$ s $^{-1}$)
December–February mean

Mean = 1.94 ng[S] m $^{-2}$ s $^{-1}$

Fig.3(c)
Climatological DMS emisisons (ng[S] m $^{-2}$ s $^{-1}$)
June–August mean

Mean = 2.15 ng[S] m $^{-2}$ s $^{-1}$

Fig.3(d)
Interactive DMS emisisons (ng[S] m $^{-2}$ s $^{-1}$)
June–August mean

Mean = 1.08 ng[S] m $^{-2}$ s $^{-1}$